Blockchain-Assisted Homomorphic Encryption Approach for Skin Lesion Diagnosis using Optimal Deep Learning Model

Kandasamy Rajeshkumar
Department of Computer and Information Science, Annamalai University, India
krajesh2000@gmail.com (corresponding author)

Chidambaram Ananth
Department of Computer and Information Science, Annamalai University, India
ananth.prog@gmail.com

Natarajan Mohananthini
Department of Electrical and Electronics Engineering, Muthayammal Engineering College, India
mohananthini@yahoo.co.in

Received: 21 December 2022 | Revised: 9 January 2023 | Accepted: 17 January

 DOI: https://doi.org/10.48084/etasr.5594

ABSTRACT

Blockchain (BC) and Machine learning (ML) technologies have been investigated for potential applications in medicine with reasonable success to date. On the other hand, as accurate and early diagnosis of skin lesion classification is essential to gradually increase the survival rate of the patient, Deep-Learning (DL) and ML technologies were introduced for supporting dermatologists to overcome these challenges. This study designed a Blockchain Assisted Homomorphic Encryption Approach for Skin Lesion Diagnosis using an Optimal Deep Learning (BHESKD-ODL) model. The presented BHESKD-ODL model achieves security and proper classification of skin lesion images using BC to store the medical images of the patients to restrict access to third-party users or intruders. In addition, the BHESKD-ODL method secures the medical images using the mayfly optimization (MFO) algorithm with the Homomorphic Encryption (HE) technique. For skin lesion diagnosis, the proposed BHESKD-ODL method uses pre-processing and the Adam optimizer with a Fully Convolutional Network (FCN) based segmentation process. Furthermore, a radiomics feature extraction with a Bidirectional Recurrent Neural Network (BiRNN) model was employed for skin lesion classification. Finally, the Red Deer Optimization (RDO) algorithm was used for the optimal hyperparameter selection of the BiRNN approach. The experimental results of the BHESKD-ODL system on a benchmark skin dataset proved its promising performance in terms of different measures.

Keywords-blockchain; smart healthcare; image encryption; deep learning; skin lesion classification

I. INTRODUCTION

Today, innovative technologies such as the Internet of Things (IoT) and big data have promoted innovations in healthcare worldwide [1], as they contribute to the development of smart healthcare systems that improve the experience of medical services. Smart healthcare is based on the electronic health and medical records of residents, integrated with information technologies, namely Cloud Computing (CC), IoT, big data, Artificial Intelligence (AI), and mobile communications that are used to develop different systems [2], namely humanized health management systems and convenient medical service systems. Furthermore, Blockchain (BC) and Machine Learning (ML) technologies have affected a wide range of scientific and industrial applications. The security, traceability, decentralization, and transparency of the ML and BC technologies enable the medical sector to upgrade and optimize different aspects, such as customer file management, customer health management [3], information system management, and medical insurance management, in addition to improving the efficacy across various applications [4]. Skin cancer is the most common form of cancer in the world [5]. Awareness of new or changing skin growths or spots, especially those that look unusual, must be assessed. The physician must assess progressive change or any new lesion in its appearance (color, size, or shape) [6-8].

This study designed a Blockchain Assisted Homomorphic Encryption Approach for Skin Lesion Diagnosis using an Optimal Deep Learning (BHESKD-ODL) model. The proposed BHESKD-ODL model uses BC to store the medical images of patients to restrict access to third-party users or intruders. In addition, the BHESKD-ODL model secures the medical images using the Mayfly Optimization (MFO) algorithm with the Homomorphic Encryption (HE) technique. For skin lesion diagnosis, the presented BHESKD-ODL method uses pre-processing and the Adam optimizer with a Fully Convolutional Network (FCN)-based segmentation process. Moreover, a radiomics feature extraction with a Bidirectional Recurrent Neural Network (BiRNN) was employed for skin lesion classification. Finally, the Red Deer Optimization (RDO) algorithm was used for the optimal hyperparameter selection of the BiRNN algorithm. The BHESKD-ODL model was experimentally tested on a benchmark skin dataset.

II. RELATED WORKS

A reliable method was proposed in [9] for skin cancer diagnosis using dermoscopy images for enriching the diagnostic abilities and visual perception of medical professionals for discriminating between malignant and benign lesions. In [10], an effective version of the recently formulated opposition-based golden jackal optimizer (IGJO) was modeled. In [11], a new automated CAD system for skin lesion classifier was presented, having high accuracy and low computational complexities. In [12], a novel analysis method for unsupervised skin melanoma removal was presented. In [13], the lesion segmenting approach was modeled as a Markov decision process, solving it by training an agent for segmenting regions utilizing a deep RL method, learned in continual action space, and utilizing the deep deterministic policy gradient technique. In [14], a new hybrid ML method for the detection of melanoma was proposed. This method used traditional ML approaches, including XGBoost supervised ML, CNNs, and EfficientNet. In [15], a potential skin cancer detection method was proposed, named Fractional Student Psychology Based Optimization-based Deep Q Network (FSPBO-based DQN), in a wireless network scenario. At first, an image was given to the preprocessing stage, where a Type II fuzzy system and the cuckoo search optimized (T2FCS) method were used to eliminate the noise of images. In [16], fairness problems in Swarm Learning (SL) were inspected. SL is a fresh edge-computing related decentralized ML method that is devised for heterogeneous illnesses recognition in precision medicine. Although several models are available in the literature, most studies did not focus on hyperparameter tuning and optimal key generation process.

III. THE PROPOSED MODEL

In this study, a secure automated skin lesion diagnosis model was designed, named BHESKD-ODL, that uses BC to securely store medical images of patients to restrict access to third-party users or intruders. In addition, the BHESKD-ODL method applied HE with the MFO-based optimal key generation process to achieve security. For skin lesion diagnosis, the presented BHESKD-ODL method used pre-processing and the Adam optimizer with FCN-based segmentation, radiomics feature extraction, BiRNN-based classification, and RDO-based hyperparameter tuning. Figure 1 shows the general procedure of the BHESKD-ODL approach.

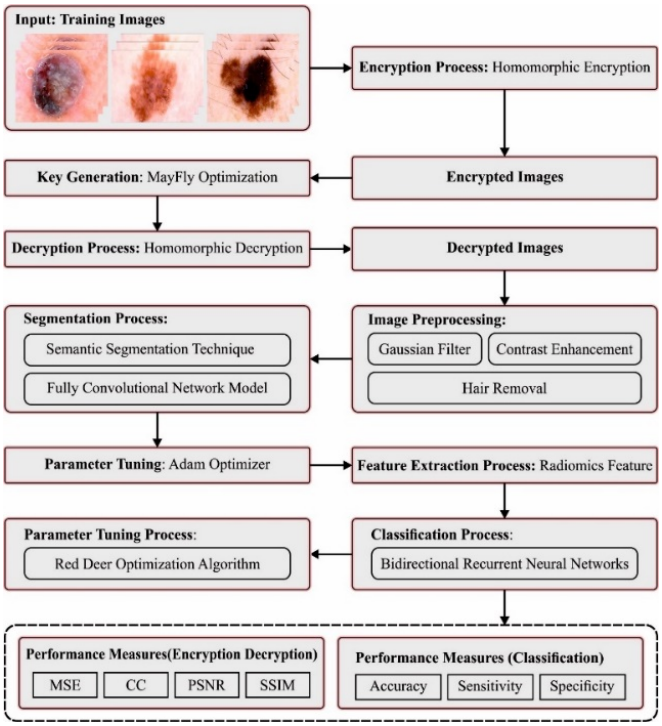

Fig. 1. General procedure of the BHESKD-ODL system.

A. Blockchain (BC)

This study used Blockchain (BC) to store images of patient skin lesions to make them inaccessible to third parties, due to the higher privacy and security requirements of medical information [17]. Hyperledger Fabric was used for saving these kinds of responses before being sent back to the user. Every reply in peers is gathered by the user and can be sent to the "orderer". During this case, every transaction is well-arranged by the orderer in ascending order and then designed to block.

B. Image Encryption using the Optimal HE Technique

The HE method was used to encrypt the medical images. In the cryptography field, the term HE describes the kind of encryption capable of performing specific computable functions on cipher images. A homomorphic function used to cipher images provides a similar (after decryption) outcome as applying the function to the original unencrypted information.

Considering m_1 and m_2 as messages, c_1 and c_2 indicate the corresponding cipher images. The operation $\dotplus$ in an additive HE generates the cipher image $c_+ \leftarrow c_1 \dotplus c_2$ that could be decrypted to m_1+m_2. Likewise, for $\times$ in multiplicative HE, it provides the $c_\times \leftarrow c_1 \times c_2$ cipher image that is decrypted to $m_1 \cdot m_2$. The HE obtains c_+ and c_x cipher images, without the knowledge of m_1 and m_2. Traditional encryption could not calculate m_1+m_2 and $m_1 m_2$ without decrypting c_1 and c_2 at first, once the user sacrifices privacy. The MFO algorithm was used for the optimal key generation process. Mayflies (MFs) in

swarming would split into individual females and males for the MFO [18]. Male MFs are continuously vigorous, since they are superior in improvement. The parameters in the MFO are similar to those of PSO, as the location is changed based on the existing velocity $v(t)$ and positions $p_i(t)$ at a given number of iterations. Every female and male MF use (1) for updating their location. At the same time, the velocity is upgraded in different forms.

$$p_i(t+1) = p_i(t) + v_i(t+1) \quad (1)$$

In the course of cycles, male creatures in Swarming Intelligence (SI) will continue to the subjugation or exploring processes. The velocity would be adjusted based on the present fitness value $f(x)$ and the better fitness value in the historical movement (xh_i). If $(x_i)>f(xh_i)$, the velocity of male MFs' is upgraded based on the existing velocity, the separation amongst them, and the global optima position. The preceding better movement is formulated as follows:

$$v_i(t+1) = g \cdot v_i(t) + \alpha_1 e^{-\beta\gamma_p^2}[\chi_{h_i} - \chi_{i(t)}] + \alpha_2 e^{-\beta\gamma_g^2}[x_g - \chi_i(t)] \quad (2)$$

where g represents the parameter that exponentially reduced from the highest to the lowest amount, and a_1, a_2, and β denote the constants for balancing the value. The Cartesian spacing amongst organisms and their prior better option, the global best location in SI, can be represented as γ_p and γ_g. The Cartesian distance is formulated by:

$$\|_{x_i} - x_j\| = \sqrt{\sum_{k=1}^{n}(x_{ik} - x_{jk})^2} \quad (3)$$

On the other hand, if $(x_i)<f(xh_i)$, the male MFs will update the speed from the existing location through an unsystematic dance factor d:

$$v_i(t+1) = g \cdot v_j(t) + d \cdot \gamma_1 \quad (4)$$

where the indiscriminate quantity in even designation and dissemination from the range [1, 1] is denoted by γ_1. The initial mate in the MFO technique can be the best male and female MFs, the second robust male and female MFs can be the second mate, and so on. Consequently, in the i-th female MFs, if $(y_i)<f(x_i)$, it can be formulated as:

$$v_i(t+1) = g \cdot v_i(t) + \alpha_3 e^{-\beta\gamma_{mf}^2}\left[x_{i(t)} - y_i(t)\right] \quad (5)$$

The Cartesian distance can be denoted as γ_m. If $(y_i)<f(x_i)$, the female MFs adjust the velocity until the present one runs through further dance coefficients fl, given by:

$$v_i(t) = g \cdot v_i(t) + fl \cdot \gamma_2 \quad (6)$$

In (6), γ_2 is the indiscriminate quantity in even designated and dissemination from the range [1, 1]. The offspring develops at a randomized rate from the mother, formulated by:

$$offspring1 = L \times male + (1-L) \times female \quad (7)$$

$$offspring2 = L \times female + (1-L) \times male \quad (8)$$

The MFO algorithm generates a fitness function for the HE technique. The maximization of the Peak Signal-to-Noise Ratio (PSNR) is considered the fitness function:

$$Fitness = \max\{PSNR\} \quad (9)$$

C. Skin Lesion Classification

The lesion classification process uses image preprocessing, optimal FCN-based segmentation, BiRNN-based classification, and RDO-based hyperparameter tuning.

1) Image Preprocessing

At the initial stage, the BHESKD-ODL method uses Gaussian Filtering (GF) for noise removal [19]. GF is linear smooth filtering, whereas the weight selected to smooth is based on the summary of the Gaussian functions. GF in the non-stop space is determined by:

$$h(m,n) = \left(\frac{1}{\sqrt{2\pi\sigma}} e^{-\frac{m^2}{2\sigma^2}}\right) \times \left(\frac{1}{\sqrt{2\pi\sigma}} e^{-\frac{n^2}{2\sigma^2}}\right) \quad (10)$$

GF is an impulse response:

$$g(x) = \sqrt{\frac{a}{\pi}} e^{-ax^2} \quad (11)$$

This formula can be also expressed with Standard Deviation (SD) as a parameter:

$$g(x) = \frac{1}{\sqrt{2\pi.\sigma}} \varepsilon^{\frac{x^2}{2\sigma^2}} \quad (12)$$

Then, the CLAHE technique was used for the contrast enhancement process. CLAHE is a kind of Adaptive Histogram Equalization (AHE) that deals with the over-amplification of the contrast. CLAHE works on smaller image regions, named tiles, instead of the whole image. Lastly, inpainting technology is applied for hair removal procedures in the skin region.

2) Image Segmentation

The FCN method is used to segment the skin lesion regions in dermoscopy images [20]. Every layer of the dataset in a ConvNet is a 3D array of size $h \times w \times d$, where h and w indicate the spatial dimension, and d indicates the channel or feature dimensions. The initial layer is the image with an $h \times w$ size and d color channels. ConvNet is based on translation invariance. The fundamental elements (activation, convolution, and pooling functions) operated on local input regions and were only based on relative spatial coordinates. Considering x_{ij} for the data vector at the (i, j) position in a specific layer, the data vector y_{ij} for the subsequent layers can be given by:

$$y_{ij} = f_{ks}(\{x_{si+\delta i, sj+\delta j}\}_{0 \le \delta i, \delta j \le k}) \quad (13)$$

where k indicates the kernel size, s represents the subsampling or stride factors, and f_{ks} defines the type of layer: a matrix multiplication for average pooling or convolution, a spatial max for max pooling, component-wise non-linearity for the activation function, etc., for other kinds of layers. This functional procedure can be preserved in composition, with kernel size and stride following the transformation rules:

$$f_{ks} o g_{k's'} = (fog)_{k'+(k-1)s', ss'} \quad (14)$$

While a deep net calculates a non-linear function, a net with only layers of these forms computes a non-linear filter that is termed a full convolution or deep filter network. The Adam optimizer was applied for the parameter tuning of the FCN, to improve optimization and convergence behavior [21]. This

method produces smooth variation with lower memory requirements and effectual computational efficiency. Based on Adam, the bias is formulated by:

$$\theta_l = \theta_{l-1} - \frac{\alpha \hat{q}_l}{\sqrt{\hat{m}l+\varepsilon}} \quad (15)$$

where α is the step size, $\hat{q}_l$ indicates corrected bias, $\hat{m}_l$ refers to the bias-corrected second-moment evaluation, ε signifies the constant, and θ_{l-1} represents the parameter at the prior time instant (*l-1*). The corrected bias of the first-order moment was formulated by:

$$\hat{q}_l = \frac{q_l}{(1-\eta_1^l)} \quad (16)$$

$$\hat{q}_l = \eta_1 q_{l-1} + (1-\eta_1) G_l^1 \quad (17)$$

The corrected bias of the second-order moment is:

$$\hat{m} = \frac{ml}{(1-\eta_2^l)} \quad (18)$$

$$\hat{m}_l = \eta_2 m_{l-1} + (1-\eta_2) H_l^2 \quad (19)$$

$$H_l = \nabla_\theta 1oss(\theta_{l-1}) \quad (20)$$

3) Feature Extraction

At this stage, radiomic features are extracted from the dermoscopy images. The radiomic features are derived by an in-house software, using Python's skicit-learn package and PyRadiomics [22]. Shape, texture, and intensity are the 3 evaluated types of characteristics. Nineteen intensity-based features and 26 shape-based features can be extracted for every extraction setting (filter, width, contour, and bin). Nineteen distinctive settings could be permutations of 2 contours (Gold and HGG), two filters (LoG and original), bandwidth (2, 4, 8, 16), and 1450 total amount of derived radiomics imaging features.

4) Image Classification using the Optimal BiRNN Model

At this stage, the BiRNN approach was used for the classifier of skin lesion images. A bi-directional RNN is an integration of two RNNs training the network in opposite directions, one from the start to the end of the sequence, and the other from the end to the start [23]. BiRNN analyzes a future event by not limiting the learning model to historical and current. As the bi-directional state modeling has improved results over the uni-state modeling in relation learning, a bi-directional state modeling method was used where $\overleftarrow{h_0}$ are the backward neuron activation models $P(h_t|\delta_t, h_T, \cdots, h_1)$ and $\overrightarrow{h_T}$ are the forward neuron activation $P(h_t|\delta_t, h_0, \cdots, h_{T-1})$. Then, implementing the *softmax* procedure, the maximum probability of the sample is discovered through the objective function. Finally, the RDO algorithm is used for the optimal hyperparameter tuning of the BiRNN model. Like other meta-heuristics, the RDO begins with a random population that is a counterpart of RD [24]. The primary population for RD is generated as follows:

$$RD = X1, X2, X3, \ldots, X_{Nvar} \quad (21)$$

Next, the fitness of every individual in the population can be evaluated by:

$$Value = f(RD) = f(X1, X2, X3, \ldots, X_{Nvar}) \quad (22)$$

Male RD is trying to increase the grace by roaring. A $resdlproV_i$ process might fail or succeed. Particularly, male RDs are the better option. This process tries to find the neighbors of the solution, concerning the solution space. When the objective function of the neighbors is male *RD*, it is replaced by the previous one if it is superior to the prior male *RD*, and it can be formulated as follows:

$$male_{new} = \begin{cases} male_{old} + a_1((UB-LB) * a_2 + LB), if\ a_3 \geq 0.5 \\ male_{old} - a_1((UB-LB) * a_2 + LB), if\ a_3 < 0.5\ is\ less\ than\ 0 \end{cases} \quad (23)$$

where *UB* and *LB* denote the upper and the lower boundaries of the problem to develop a relevant male neighborhood solution. The existing location of male *RD* is $male_{old}$, and its following location is $male_{new}$. Based on randomization, $a1$, $a2$, and $a3$ are the 3 phases of the roaring procedure, which is a uniform distribution of a random number within [0,1]. N_c can be evaluated using:

$$N_C = round(\gamma . N_{male}) \quad (24)$$

where N_c indicates the number of male commanders in the population, γ is a randomly generated value within [0,1], and N_{male} indicates the number of overall males. Note that γ represents the initial value of the model which ranges from 0 to 1. The number of stags can be evaluated using:

$$N_s = N_{male} - N_C \quad (25)$$

The fighting strategy can be formulated using:

$$new1 = \frac{C+S}{2} + b_1\big((UB-LB) * b_2 + LB\big) \quad (26)$$

$$new_2 = \frac{C+S}{2} - b_1\big((UB-LB) * b_2 + LB\big) \quad (27)$$

where new_1 and new_2 indicate the new solutions proposed by the fighting strategy, *C* and *S* denote the stags and commanders, respectively, *UB* and *LB* indicate the upper and lower boundaries of the problem, and similarly, b_1 and b_2 indicate the upper and lower boundaries of the search space, with uniformly distributed number ranges from 0 to 1. Considering the four options *C*, *S*, new_1, and new_2, only the finest one regarding the OF is selected.

Hinds were used amongst commanders to form a group of harems as follows:

$$V_n = v_n - \max v_i \quad (28)$$

where V_n is the normalized value of *n*-th commander's power (VF), and v_n is the power of the *n*-th commander (OF). The normalized power of the commander is calculated by:

$$P_n = \left| \frac{V_n}{\sum_{i=1}^{a_i} V_i} \right| \quad (29)$$

and the number of hinds of the harem is given by:

$$N.harem_n = round(P_n \cdot N_{hind}) \quad (30)$$

where N_{hind} is the overall amount of hinds. The fitness selection is an essential factor in the RDO algorithm. Solution encoding was used to assess the aptitude (goodness) of the candidate solution. The accuracy value was the core condition used to design a fitness function:

$$Fitness = \frac{TP}{TP+FP} \quad (31)$$

where TP and FP are the true and false positive values, respectively.

IV. RESULTS AND DISCUSSION

The skin lesion classification of the BHESKD-ODL system was tested using the ISIC database [25]. The BHESKD-ODL approach was simulated using Python 3.6.5 and an i5-8600K/16GB/GeForce 1050Ti 4GB PC. Figure 2 shows some examples of the visualization of images of skin lesions. The first row shows the original images, the second row demonstrates the encrypted images, the third row illustrates the decrypted images, the fourth row exhibits the pre-processing images, and the fifth row defines the segmented images.

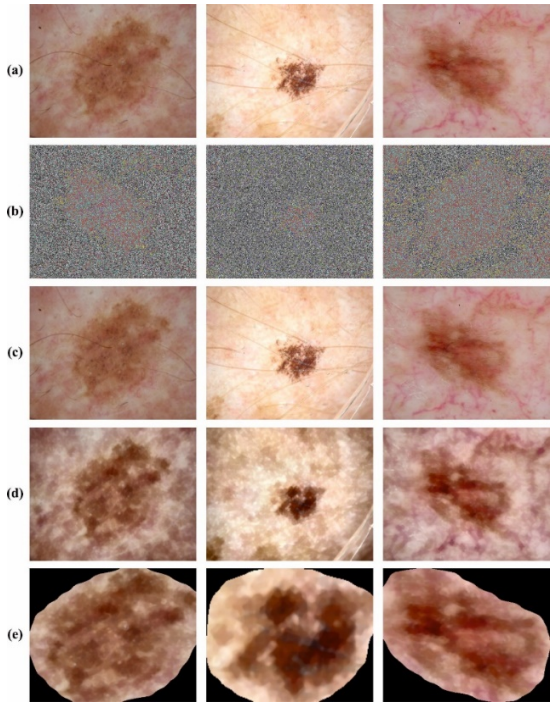

Fig. 2. (a) Original images, (b) encrypted images, (c) decrypted images, (d) preprocessed images, (e) segmented images.

Table I shows the encryption results of the BHESKD-ODL with other methods, in terms of MSE and PSNR. The results show that the BHESKD-ODL model achieved excellent performance with maximal PSNR and minimal MSE. Based on MSE, the BHESKD-ODL model reached 0.0908, while the HOCE-ECC, GO-ECC, PSO-ECC, and CS-ECC models had increased MSEs.

TABLE I. MSE AND PSNR RESULTS OF BHESKD-ODL AND OTHER APPROACHES

Methods	MSE	PSNR
BHESKD-ODL	0.0908	58.6095
HOCE-ECC	0.1190	57.3800
GO-ECC	0.1340	56.8600
PSO-ECC	1.1450	47.5400
CS-ECC	1.2780	47.0700

Table II shows an overall comparison analysis of the BHESKD-ODL method with recent DL approaches [26-27]. The results show that BHESKD-ODL reached increased performance over the other models. These results demonstrate that the BHESKD-ODL model showed secure skin lesion classification performance.

TABLE II. COMPARATIVE ANALYSIS OF BHESKD-ODL WITH RECENT DL METHODS

Methods	Accuracy	Sensitivity	Specificity
BHESKD-ODL	99.54	99.61	99.92
Inception-V3	85.70	86.46	86.06
VGGNet	78.60	79.60	79.68
AlexNet-VGGNet	79.90	80.35	80.47
U-Net	80.00	79.43	78.92
Resnet50	83.60	84.89	85.14
Resnet50-Inception	84.10	84.25	84.09

V. CONCLUSION

This paper presented the design of an automated and secure skin lesion diagnosis model, named BHESKD-ODL. The BHESKD-ODL model uses blockchain technology to securely store patient medical images and restrict access to third-party users or intruders. Additionally, the BHESKD-ODL method applies homographic encryption with a Mayfly optimization-based key generation process to achieve security. For skin lesion diagnosis, the presented BHESKD-ODL model uses preprocessing and the Adam optimizer with FCN-based segmentation, radiomics feature extraction, BiRNN-based classification, and RDO-based hyperparameter tuning. The experimental evaluation of the BHESKD-ODL method used a benchmark skin dataset. A detailed comparison study showed the promising performance of the BHESKD-ODL model concerning distinct measures. In the future, hybrid metaheuristic algorithms can be employed to improve the performance of the BHESKD-ODL model.

REFERENCES

[1] A. Selvia, V. N. Prakash, N. Saravanan, B. Jawahar, and V. Karthick, "Skin Lesion Detection Using Feature Extraction Approach," *Annals of the Romanian Society for Cell Biology*, pp. 3939–3951, Apr. 2021.

[2] J. Saeed and S. Zeebaree, "Skin Lesion Classification Based on Deep Convolutional Neural Networks Architectures," *Journal of Applied Science and Technology Trends*, vol. 2, no. 01, pp. 41–51, Mar. 2021, https://doi.org/10.38094/jastt20189.

[3] M. K. Islam, C. Kaushal, and M. A. Amin, "Smart Home-Healthcare for Skin Lesions Classification with IoT Based Data Collection Device." TechRxiv, Nov. 08, 2021, https://doi.org/10.36227/techrxiv.16870729.v1.

[4] S. Joseph and O. O. Olugbara, "Preprocessing Effects on Performance of Skin Lesion Saliency Segmentation," *Diagnostics*, vol. 12, no. 2, Feb. 2022, Art. no. 344, https://doi.org/10.3390/diagnostics12020344.

[5] Y. Slimani and R. Hedjam, "A Hybrid Metaheuristic and Deep Learning Approach for Change Detection in Remote Sensing Data," *Engineering, Technology & Applied Science Research*, vol. 12, no. 5, pp. 9351–9356, Oct. 2022, https://doi.org/10.48084/etasr.5246.

[6] N. C. Kundur and P. B. Mallikarjuna, "Deep Convolutional Neural Network Architecture for Plant Seedling Classification," *Engineering, Technology & Applied Science Research*, vol. 12, no. 6, pp. 9464–9470, Dec. 2022, https://doi.org/10.48084/etasr.5282.

[7] S. Khan, I. Ali, F. Ghaffar, and Q. Mazhar-ul-Haq, "Classification of Macromolecules Based on Amino Acid Sequences Using Deep

Learning," *Engineering, Technology & Applied Science Research*, vol. 12, no. 6, pp. 9491–9495, Dec. 2022, https://doi.org/10.48084/etasr.5230.

[8] C. Ananth, M. Karthikeyan, and N. Mohananthini, "A secured healthcare system using private blockchain technology," *Journal of Engineering Technology*, vol. 6, no. 2, pp. 42–54, Jul. 2018.

[9] P. Thapar, M. Rakhra, G. Cazzato, and M. S. Hossain, "A Novel Hybrid Deep Learning Approach for Skin Lesion Segmentation and Classification," *Journal of Healthcare Engineering*, vol. 2022, Apr. 2022, Art. no. e1709842, https://doi.org/10.1155/2022/1709842.

[10] E. H. Houssein, D. A. Abdelkareem, M. M. Emam, M. A. Hameed, and M. Younan, "An efficient image segmentation method for skin cancer imaging using improved golden jackal optimization algorithm," *Computers in Biology and Medicine*, vol. 149, Oct. 2022, Art. no. 106075, https://doi.org/10.1016/j.compbiomed.2022.106075.

[11] W. Salma and A. S. Eltrass, "Automated deep learning approach for classification of malignant melanoma and benign skin lesions," *Multimedia Tools and Applications*, vol. 81, no. 22, pp. 32643–32660, Sep. 2022, https://doi.org/10.1007/s11042-022-13081-x.

[12] R. Rout and P. Parida, "A novel method for melanocytic skin lesion extraction and analysis," *Journal of Discrete Mathematical Sciences and Cryptography*, vol. 23, no. 2, pp. 461–473, Feb. 2020, https://doi.org/10.1080/09720529.2020.1728900.

[13] U. A. Usmani, J. Watada, J. Jaafar, I. A. Aziz, and A. Roy, "A Reinforcement Learning Algorithm for Automated Detection of Skin Lesions," *Applied Sciences*, vol. 11, no. 20, Jan. 2021, Art. no. 9367, https://doi.org/10.3390/app11209367.

[14] S. Zhang, S. Huang, H. Wu, Z. Yang, and Y. Chen, "Intelligent Data Analytics for Diagnosing Melanoma Skin Lesions via Deep Learning in IoT System," *Mobile Information Systems*, vol. 2021, Nov. 2021, Art. no. e8700506, https://doi.org/10.1155/2021/8700506.

[15] K. S. Kumar, N. Suganthi, S. Muppidi, and B. S. Kumar, "FSPBO-DQN: SeGAN based segmentation and Fractional Student Psychology Optimization enabled Deep Q Network for skin cancer detection in IoT applications," *Artificial Intelligence in Medicine*, vol. 129, Jul. 2022, Art. no. 102299, https://doi.org/10.1016/j.artmed.2022.102299.

[16] D. Fan, Y. Wu, and X. Li, "On the Fairness of Swarm Learning in Skin Lesion Classification," in Clinical Image-Based Procedures, Distributed and Collaborative Learning, Artificial Intelligence for Combating COVID-19 and Secure and Privacy-Preserving Machine Learning, Strasbourg, France, 2021, pp. 120–129, https://doi.org/10.1007/978-3-030-90874-4_12.

[17] E. A. Mantey, C. Zhou, S. R. Srividhya, S. K. Jain, and B. Sundaravadivazhagan, "Integrated Blockchain-Deep Learning Approach for Analyzing the Electronic Health Records Recommender System," *Frontiers in Public Health*, vol. 10, 2022, https://doi.org/10.3389/fpubh.2022.905265.

[18] P. Subramani, S. Mani, W.-C. Lai, and D. Ramamurthy, "Sustainable Energy Management and Control for Variable Load Conditions Using Improved Mayfly Optimization," *Sustainability*, vol. 14, no. 11, Jan. 2022, Art. no. 6478, https://doi.org/10.3390/su14116478.

[19] S. Bharati, T. Z. Khan, P. Podder, and N. Q. Hung, "A Comparative Analysis of Image Denoising Problem: Noise Models, Denoising Filters and Applications," in *Cognitive Internet of Medical Things for Smart Healthcare: Services and Applications*, A. E. Hassanien, A. Khamparia, D. Gupta, K. Shankar, and A. Slowik, Eds. Cham, Switzerland: Springer International Publishing, 2021, pp. 49–66.

[20] J. Long, E. Shelhamer, and T. Darrell, "Fully Convolutional Networks for Semantic Segmentation," presented at the Proceedings of the IEEE Conference on Computer Vision and Pattern Recognition, 2015, pp. 3431–3440.

[21] K. K. Chandriah and R. V. Naraganahalli, "RNN / LSTM with modified Adam optimizer in deep learning approach for automobile spare parts demand forecasting," *Multimedia Tools and Applications*, vol. 80, no. 17, pp. 26145–26159, Jul. 2021, https://doi.org/10.1007/s11042-021-10913-0.

[22] J. Qian *et al.*, "Prediction of MGMT Status for Glioblastoma Patients Using Radiomics Feature Extraction From 18F-DOPA-PET Imaging," *International Journal of Radiation Oncology*Biology*Physics*, vol. 108, no. 5, pp. 1339–1346, Dec. 2020, https://doi.org/10.1016/j.ijrobp.2020.06.073.

[23] L. E. Yerimah, S. Ghosh, Y. Wang, Y. Cao, J. Flores-Cerrillo, and B. W. Bequette, "Process prediction and detection of faults using probabilistic bidirectional recurrent neural networks on real plant data," *Journal of Advanced Manufacturing and Processing*, vol. 4, no. 4, 2022, Art. no. e10124, https://doi.org/10.1002/amp2.10124.

[24] A. M. Tadkal and S. V Mallapur, "Red deer optimization algorithm inspired clustering-based routing protocol for reliable data dissemination in FANETs," *Materials Today: Proceedings*, vol. 60, pp. 1882–1889, Jan. 2022, https://doi.org/10.1016/j.matpr.2021.12.527.

[25] "ISIC Challenge Dataset." International Skin Imaging Collaboration, 2020, [Online]. Available: https://challenge2020.isic-archive.com/.

[26] U. Padmavathi and N. Rajagopalan, "Blockchain Enabled Emperor Penguin Optimizer Based Encryption Technique for Secure Image Management System," *Wireless Personal Communications*, vol. 127, no. 3, pp. 2347–2364, Dec. 2022, https://doi.org/10.1007/s11277-021-08800-w.

[27] W. Gouda, N. U. Sama, G. Al-Waakid, M. Humayun, and N. Z. Jhanjhi, "Detection of Skin Cancer Based on Skin Lesion Images Using Deep Learning," *Healthcare*, vol. 10, no. 7, Art. no. 1183, Jul. 2022, https://doi.org/10.3390/healthcare10071183.